Available online at www.sciencedirect.com

ScienceDirect

journal homepage: http://www.elsevier.com/locate/jab

Original Research Article

Self-assembly of carrageenin–$CaCO_3$ hybrid microparticles on bacterial cellulose films for doxorubicin sustained delivery

Maximiliano L. Cacicedo [a], *Karina Cesca* [b], *Valeria E. Bosio* [a], *Luismar M. Porto* [b], *Guillermo R. Castro* [a,*]

[a] *Nanobiomaterials Laboratory, Institute of Applied Biotechnology (CINDEFI, CONICET CCT La Plata), Department of Chemistry, School of Sciences, Universidad Nacional de La Plata, Calle 47 y 115, CP 1900, Ciudad de La Plata, Argentina*
[b] *Integrated Technologies Laboratory (InteLAB), CTC/EQA, Universidad Federal de Santa Catarina, Florianopolis, Brazil*

ARTICLE INFO

Article history:
Received 13 November 2014
Received in revised form
6 March 2015
Accepted 9 March 2015
Available online 1 April 2015

Keywords:
Self-assembly
Nanocomposites
Hybrid microparticles
Bacterial cellulose
Doxorubicin
Smart chemotherapy

ABSTRACT

Stereospecific nucleation of mesoporous hybrid microspheres composed of $CaCO_3$ and carrageenan was appended to one side of bacterial cellulose membrane synthesized in static cultures of *Gluconacetobacter hansenii* to develop an implantable drug delivery device. The synthesis of the hybrid microparticles proceeds by self-assembly mechanism in the presence of calcium and contains tailorable amounts of doxorubicin. However, in the absence of the particles, doxorubicin was distributed along the BC film, but without control release of drug. Infrared spectroscopy, confocal and scanning electron microscopies analyses demonstrate that the doxorubicin is entrapped inside the hybrid particles with approximately 80% drug loading compared to the 11% obtained for native bacterial cellulose. Doxorubicin content in the hybrid particles can be increased by a factor of 10 (from 258.6 to 2586.3 nmol ml^{-1}), and also by the quantities of particles regulated by the $CaCO_3$–carrageenan content and the physicochemical microenvironment. The hybrid BC system can be considered as smart device since the kinetic release of doxorubicin from the hybrid cellulose system rise from 1.50 to 2.75 μg/membrane/day when the pH decreases from 7.4 to 5.8 at 37 °C, a pathologic simulated environment. The hybrid microparticle system can be potentially used as an implantable drug delivery system for personalized oncological therapies.

Introduction

Bacterial cellulose (BC) is an extracellular hydrophilic polysaccharide constituted by β-(1→4) glucose chains and biosynthesized in the air/culture medium interface by *Gluconacetobacter hansenii* among other microorganisms (Petersen and Gatenholm, 2011). The unique nanofibrillar structure has high water content (about 99%) and displays distinctive properties such as high purity, high degree of

* Corresponding author. Tel.: +54 221 483 37 94x132/103; fax: +54 221 483 37 94x132/103.
E-mail address: grcastro@gmail.com (G.R. Castro).
1214-021X/$ – see front matter
http://dx.doi.org/10.1016/j.jab.2015.03.004

polymerization (up to 8000), high crystallinity (70–80%), and high mechanical stability (Barud et al., 2011). Particularly, BC has been widely studied for wound healing and tissue engineering (Svensson et al., 2005; Helenius et al., 2006). The development of nanocomposite films based on BC and polymers were performed based on two main strategies: BC fibrils were dissolved into an aqueous polymer based solution followed by solvent removal (Fernandes et al., 2009). Alternatively, nanocomposite films were made by the addition of the polymer solution during the growth of the BC fibrils in the microbial cell culture. Studies made on BC nanocomposites of gelatin, collagen, hyaluronic acid and alginates showed high biocompatibility in many mammalian cell cultures with the improvement of mechanical properties, cell adhesion, growth and proliferation and low immunogencity (Cai et al., 2011; Chiaoprakobkij et al., 2011; Duran Lopes et al., 2014). Also, BC was proposed as potential candidate for the development of molecular controlled release systems (Almeida et al., 2014).

Calcium carbonate is one of the most abundant materials in earth and it can be found in six different polymorphisms. Among them, vaterite is the most stable and useful to synthesize hybrid materials because of its crystal size, distribution and geometry (Beuvier et al., 2011). Several approaches were used to determine the polymorphism and morphology of $CaCO_3$ crystals including size control, shape, and oriented aggregation. Self-assembly of $CaCO_3$ on BC was developed to obtain lamellar structures for potential application in tissue engineering (Liu et al., 2013). Morphological changes of $CaCO_3$ from rhombohedral to spheroidal structures in the presence of BC made by ultrasound or microwave pulses were observed (Stoica-Guzun et al., 2013). However, these techniques are providing heterogeneous morphologies and mixed crystal structures (vaterite–calcite) of $CaCO_3$-BC nanocomposites which are not appropriate for technological purposes such as drug delivery.

Carrageenans (Cars) are linear hydrocolloids chemically composed of galactose sulfate esters and 3,6-anhydro galactose linked by α-1,3 and β-1,4 bonds. The Cars are currently used as gelling agents, thickeners, emulsifiers and stabilizers in food and pharmaceutical applications. Besides, biological activities of Cars such as anticoagulant, immunomodulatory, antiviral, antithrombotic and antitumor activities were reported (Campo et al., 2009).

Doxorubicin (Dox) is one of the most extensively used drugs in oncological therapies and administered by intravenous injections. Unfortunately, Dox is highly toxic, and the biodistribution into non-targeted cells can cause undesirable side effects in several tissues and organs (*e.g.* in heart, liver, kidneys, stomach, brain and blood cell lineages) and unwanted physiological consequences during chemotherapies such as vomiting, nausea, gastrointestinal problems, and frequently producing hallucinations and light-headedness. In recent years, drug encapsulation is offering many advantages such as: (i) the reduction of potential toxic side effects associated with the ''free'' circulating drug, (ii) the protection of the drug against *in vivo* degradation, (iii) the increase in patient comfort by avoiding repetitive bolus injection or the use of perfusion pumps, and (iv) favorable drug pharmacokinetics. Some examples of Dox-containing micro- and nano-particles, such as polymeric carriers, liposomes, and inorganic magnetic nanoparticles were recently reviewed (Tacar et al., 2012). Additionally, in previous work of our laboratory, Dox was encapsulated in nanostructured hybrid microparticles (N-hMPs) made of $CaCO_3$ and λ-Car as biopolymer template. The λ-Car-$CaCO_3$ nanocomposite was analyzed by several procedures including spectroscopic and microscopy techniques showing spherical structure and up to 95% vaterite crystal polymorphism (Bosio et al., 2014). The λ-Car-$CaCO_3$ nanocomposite microparticles are considered highly stable and smart structures because they are pH-responsive releasing the Dox at slight acid pH produced by pathological states like in presence of tumors and cancer cells (*e.g.* pH ≈ 5.8), but keeping the drug inside for more than one year in PBS (pH 7.4). Also, the λ-Car-$CaCO_3$ nanocomposite showed high Dox encapsulation with efficiency up to 83%, high surface area, small pore size, and lack of toxicity in cell cultures after 24 h (Bosio et al., 2014). Besides, from the therapeutic point of view the main challenge of the Dox administration is still related to reduce the multidirectional cytotoxic activity in several tissues and organs associated to the undesirable side effects (Tacar et al., 2012).

The FDA (Food and Drug Administration, USA) just reported the approval of four cancer drugs for patients with specific genetic characteristics which is reflecting a new trend for therapeutics: personalized medicine. Personalized Medicine can be defined as customization of the healthcare by tailoring the therapies based on the individual characteristics of the patient, pathology and needs (Anon., 2013). In addition, variable disposition and therapeutic efficacy of Dox nanoparticles particularly related to tumor microenvironment on breast cancer cell lines was recently reported. The biological heterogeneity of the tumors, made by the tumor cell diversity and the surrounding microenvironment, displayed different sensitivity to the Dox nanoparticle chemotherapies but not to free doxorubicin (Song et al., 2014). Following this line, local drug delivery offers high potentiality in the personalized cancer therapies using theranostics by combining imaging, molecular diagnosis and specific therapeutic procedures. Among the limitations of implantable therapeutic films it can be mentioned the requirements of sophisticated equipment such as scanners, and molecular biology tools to establish the tumor characteristics in order to determine the proper drug quantities to be administered, and the requirement of surgery to implant and take out the film from the patient at certain time. However, from the therapeutic point of view, the advantage of an implantable film device loaded with highly toxic drug, like doxorubicin, is advantageous since the drug administration is only local and reducing systemic Dox distribution increases not only the quality life of an oncologic patients but also the life span. Particularly, during the detection of the first oncogenic stages of solid tumors and/or after surgery which potentially allows the development of local chemotherapy which is more effective in reducing cancer recurrences and avoiding undesirable side effects of high systemic drug concentrations. Additionally, there is a controlled and prolonged drug release to ensure adequate concentration, diffusion, and uptake into cancer cells over many cycles of tumor cell division by localized therapies (Wolinsky et al., 2012).

To the best of our knowledge, this is the first report on bacterial cellulose films developed for local controlled release of drugs.

The aim of the present work was to develop a bacterial cellulose (BC) film as tailorable and implantable drug delivery device containing Dox for potential application in personalized cancer therapies. The studies were focused on the development of smart bacterial cellulose membrane containing λ-Car and $CaCO_3$ nanocomposite microparticles loaded with different amounts of Dox. The characterization of the nanocomposite BC systems was performed by infrared spectroscopy, thermogravimetric analysis, confocal and scanning electron microscopies. Analyses of Dox loading to BC membranes and *in vitro* Dox kinetic release from the matrices at different pHs were also done.

Materials and methods

Chemicals and media

Lambda carrageenan (λ-Car) was purchased from Satiagel (SKW Biosystems, Buenos Aires, Argentina). Doxorubicin (Dox, MW = 579.98) was a gift from LKM pharmaceuticals (Argentina). All other reagents used were of analytical or microbiological grade purchased from Sigma–Aldrich (St. Louis, MO) or Merck (Darmstadt).

Bacterial cellulose

The synthesis of Bacterial cellulose (BC) by *G. hansenii* (ATCC 23769) was performed in a medium containing ($g\,l^{-1}$): 25.0 mannitol, 5.0 yeast extract, 3.0 Peptone, and adjusted to pH 6.5 with 0.1 M NaOH solution before sterilization. The culture was maintained statically in 96-well plates at 30 °C for 6 days. The BC films were collected from the plates and washed with distilled water. BC purification was performed incubating the membranes in 100 mM NaOH at 50 °C for 24 h followed by successive washes with distilled water, after pH was adjusted to 7.0. Later, the BC films were sterilized by autoclaving (121 °C for 20 min).

Synthesis of the system

Hybrid matrixes of Bacterial Cellulose (BC) containing λ-Car were produced immersing the BC films into a solution containing 0.1% λ-Car for 24 h at room temperature with stirring (100 rpm). Later, films were washed twice with physiologic solution (154 mM NaCl).

BC system containing nanostructured micro-hybrid particles (N-HMPs) was developed by colloidal crystallization in presence of $CaCl_2$, glycine (Gly), Na_2CO_3 and λ-Car as follows: BC films were immersed in a vial containing 3.2% (w/v) Na_2CO_3 and 0.1% λ-Car at 25 °C for 20 min. Later, a solution containing 3.2% (w/v) $CaCl_2$ in 1.25 M Gly-NaCl buffer (pH 10.0) was poured into the vial, and stirred at 300 rpm for other 20 min. Each film was washed twice with 2 ml of distilled water followed by physiologic solution (Bosio et al., 2014).

Drug loading studies

Membrane systems were immersed into Dox solutions ranging from 0.51 to 2.59 nmols ml^{-1}) in 100 mM MES buffer (pH 6.5) and stirred at 300 rpm, 25 °C for 20 h. Dox was quantified by spectrofluorimetry (Perkin Elmer LS 50B, Japan) using λ_{exc} = 454 nm and λ_{em} = 588 nm with appropriate calibration curve.

The membranes were taken out from the vials and residual Dox was spectrofluorometrically assayed in the supernatants. Membranes were washed 3 times in 145 mM NaCl and 100 mM MES buffer (pH 6.5). The loading efficiency was evaluated as follow:

$$\text{Dox incorporation} = \frac{(\text{Dox}_0 - \text{Dox}_t)}{W_{BC}}$$

where Dox_0 and Dox_t are μmols of Doxorubicin in the solution at time zero and time t, and W_{BC}, represent the mass of BC film (grams).

Infrared spectroscopy

BC films were examined in ATR-FTIR spectrometer (Nicolet MAGNA 560), using BCTA detector. The samples were analyzed in the 4000–650 cm^{-1} spectral range with 4 cm^{-1} resolution and 64 scans. Images were processed with OMNIC software (Thermo Electron Corp., Waltham, MA).

Thermogravimetric analysis (TGA)

Dynamic thermogravimetric measurements of native and hybrid bacterial cellulose membranes were performed by using a TGA-50 model instrument (Shimadzu, Japan). Tests were run from 20 °C to 900 °C at a heating rate of 10 °C/min under N_2 atmosphere.

Confocal laser scanning microscopy (CLSM)

Fluorescence images were made using the Dox autofluorescence. Loaded and unloaded hybrid biofilms were examined by confocal microscopy (Leica model TCS SP5, Leica Microsystems CMS GmbH, Mannheim, Germany). The microscope collected 8 bit images using four detectors for fluorescent signals and a transmission detector for bright field images. Objective used was HCX PL APO CS 63.0 × 1.40 OIL UV and an emission bandwidth PMT 1: 415–485 nm (begin–end). Scanner settings were pinhole [m] 191.1 μm, and pinhole [air] 2.0 with scan mode xyz. Leica Application Suite Advanced Fluorescence (LAS AF) software was used to control the microscope and data analysis.

Scanning electron microscopy (SEM)

Samples were made by sputtering the surface with gold using a metalizer (Balzers SCD 030) obtaining layer thickness between 15 and 20 nm. Films surfaces and morphologies were observed by SEM (Philips SEM 505 model, Rochester, NY, USA), and the images processed by an image digitalizer program (Soft Imaging System ADDA II).

In vitro *drug release studies*

BC membranes were placed in 1.5 ml of 10 mM PBS buffer on 2.0-ml plastic vials at 37 °C. Samples of 500 μl were withdrawn and refilled with an equal volume of fresh buffer at defined

intervals. Dox concentration was determined by fluorescence as mentioned before. Release experiments were performed three times in duplicate or in triplicates for each system and concentration. The Dox release from the matrices was studied in the pH range of 5.8–7.4 using 10 mM phosphate buffer adjusted with 1.0 M NaOH or HCl.

Statistical analysis

All experiments were carried out at least in duplicate. Comparisons of the means were performed by analysis of variance (ANOVA) followed by two-sided Fisher's least significant difference test at the significance level of $2\alpha = 0.05$.

Results and discussion

Bacterial cellulose (BC) films produced by *G. hansenii* were cleaned and then sterilized. In preliminary assays, BC films were incubated in presence of different Dox concentrations, and some drug was absorbed on the film but no controlled release of Dox was observed (data not shown). Later, the synthesis of the nanocomposite hybrid microparticles (N-hMPs) made of $CaCO_3$ and λ-Car were performed in the presence and absence of the BC films by $CaCl_2$. The resulting N-hMPs were found appended to one the hairy side of the BC film and studied alone and on the BC film surface. The spherical shape of N-hMPs was observed by SEM showing similar structure as previously reported (Fig. 1A) (Bosio et al., 2014; Islan et al., 2014). Additionally, the SEM images of the BC membranes with or without N-hMPs revealed a ''hairy'' structure on one of the film side (Fig. 1B and C). Interestingly, the SEM pictures are showing the N-hMPs only on the BC surface indicating that the spontaneous $CaCO_3$ nucleation proceeds only at the interface of the BC film-solution. In fact, the N-hMPs showed spherical morphology of about 4 μm average diameter and appended only on one side of BC which is displaying hairy surface (Fig. 1C). The SEM images of transversal slices of BC membranes containing λ-Car-$CaCO_3$ with different magnifications are confirming the presence of the microparticles particularly on the ''hairy'' side of BC membrane surface (Fig. 2A and B). This result is indicating positive contribution of the free cellulose chains appended on the BC membrane on the N-hMP synthesis. Therefore, a novel method for the modification of BC films surface was developed.

Dox loading into the BC-λ-Car-$CaCO_3$ films did not modify the general distribution of N-hMPs and the morphology of the BC system observed by SEM (Fig. 3A and B). Based on the hydrophilicity of Dox and considering the highly polar environment of the solution made by the salts and the λ-Car characteristics, Dox will be located inside the N-hMPs

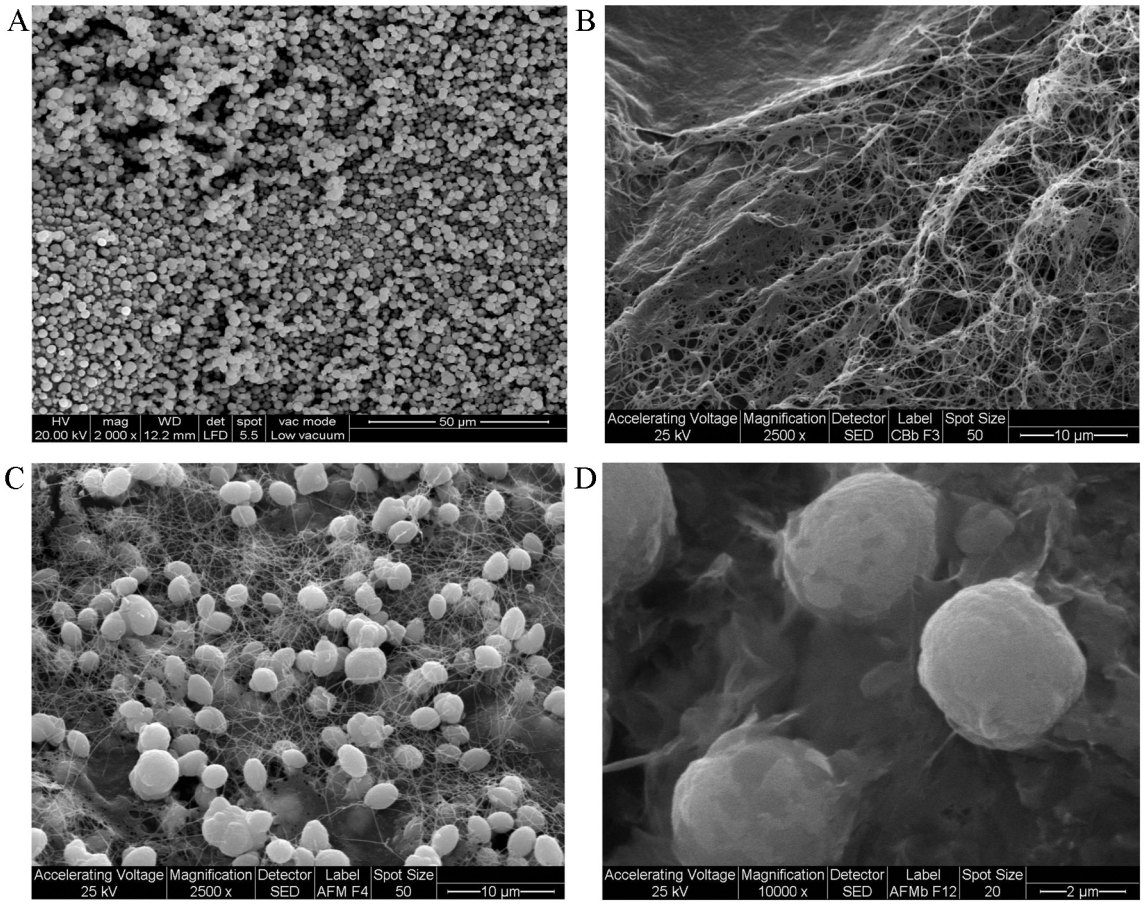

Fig. 1 – Scanning electron microscopies of λ-Car-$CaCO_3$ microparticles and bacterial cellulose (BC) membranes: (A) λ-Car-$CaCO_3$ microparticles (N-hMPs); (B) naked BC and (C and D) BC containing λ-Car-$CaCO_3$ (BC/N-hMPs).

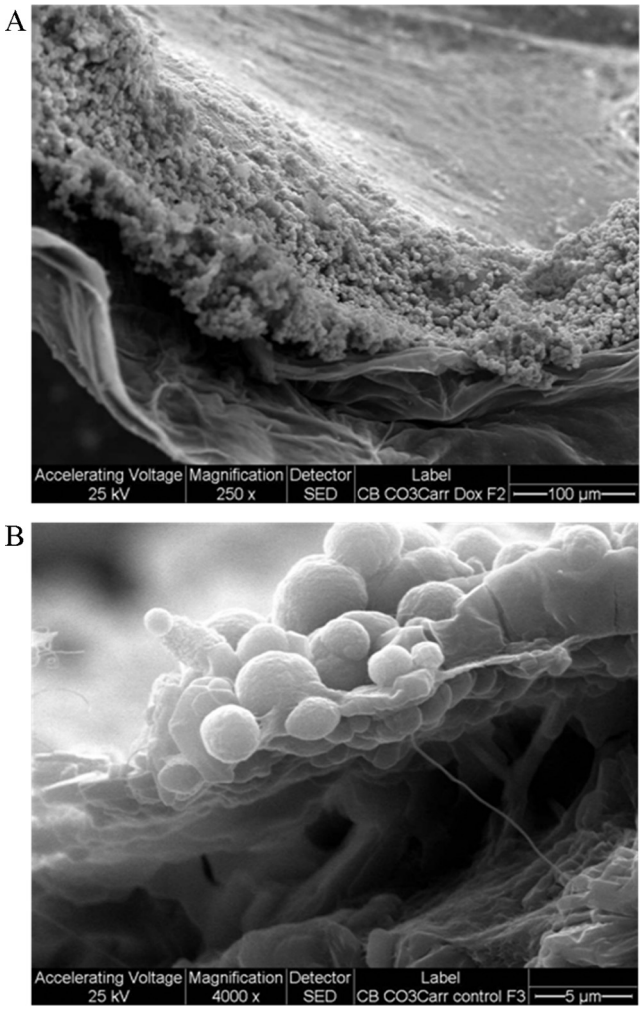

Fig. 2 – Transversal cuts of BC/N-hMPs membranes by SEM at different magnifications (A and B).

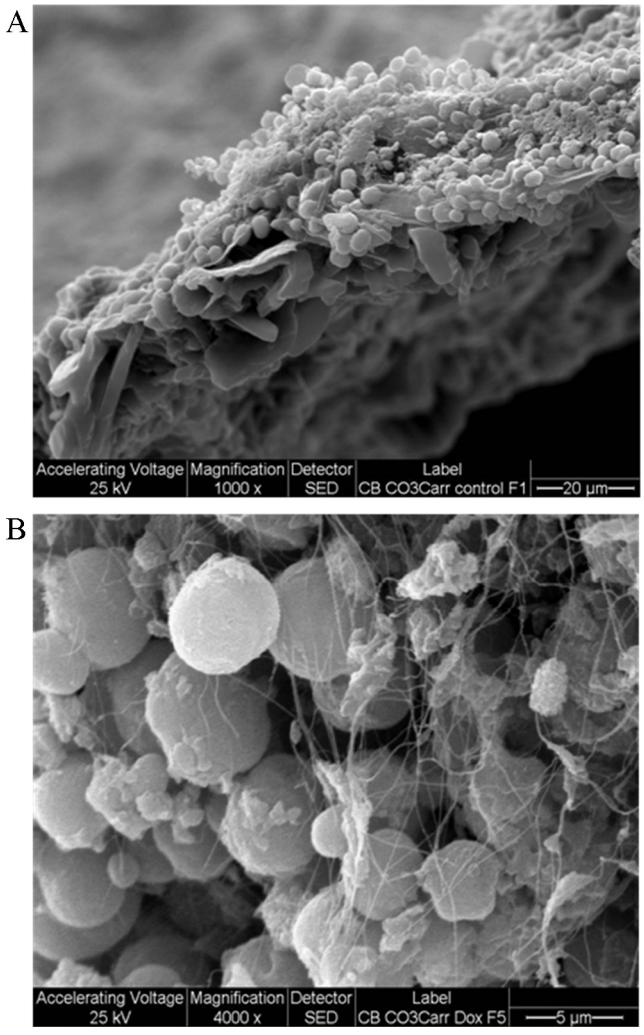

Fig. 3 – SEM images of BC/N-hMPs membranes containing Dox at different magnifications (A and B).

instead of the BC membrane. Also, the pending cellulose chains of the structure in one side of the BC membrane are providing the free hydroxyl groups which are the potential sites for λ-Car-$CaCO_3$ nucleation. The SEM images of the BC membranes at 1000× and 4000× magnification are showing cellulose thread network in where N-hMPs were trapped (Fig. 3A and B).

Thermal stability and decomposition of BC and BC N-hMP systems were analyzed by thermogravimetric analysis (TGA) (Fig. 4). Two decomposition steps were observed for unmodified bacterial cellulose and bacterial cellulose containing hybrid particles. The first step was attributed to unbound water content, observed in the temperature range from 65 °C to 100 °C showing an equal weight loss of 7% for both samples. The second step for both samples was attributed to thermal decomposition of the biomaterial. Moreover, the first derivative of the weight loss curve (DTGA) showed a shift in the decomposition temperature of biofilms, from 315.8 °C to 357.9 °C for BC and BC N-hMPs composite respectively (Fig. 4). Consequently, the thermal stability of BC was enhanced by the presence of $CaCO_3$ and also by the hybrid microparticles (see supplementary data, Fig. 1S). The change of thermal behavior of BC containing $CaCO_3$ or λ-Car $CaCO_3$ is suggesting some structural changes made by the presence of λ-Car (see supplementary data, Table 1S). Probably associated to the presence of high content of vaterite polymorphism in the $CaCO_3$ crystal, which it was attributed to the peak at 744 cm^{-1} for BC N-hMPs determined by FTIR (data not shown) (Brito et al., 2009).

Confocal microscopy was used to detect the fluorescence emitted by Dox, and consequently the drug location in the film system can be tracked (see supplementary data, Fig. 2S). The confocal images of the membranes are displayed in Fig. 5. Fig. 5A is showing a homogeneous distribution of Dox on naked BC membranes without preferred location for the drug on the film surface. When the BC was soaked in presence of λ-Car and later with Dox, some preferential fluorescent spots can be observed probably associated to the presence of the λ-Car attached to the BC membrane (Fig. 5B). Similar results were observed in presence of $CaCO_3$ (Fig. 5C), but in this case the amount of Dox loaded in the BC membrane is lower, which is probably attributed to the polar salt solution in where most of

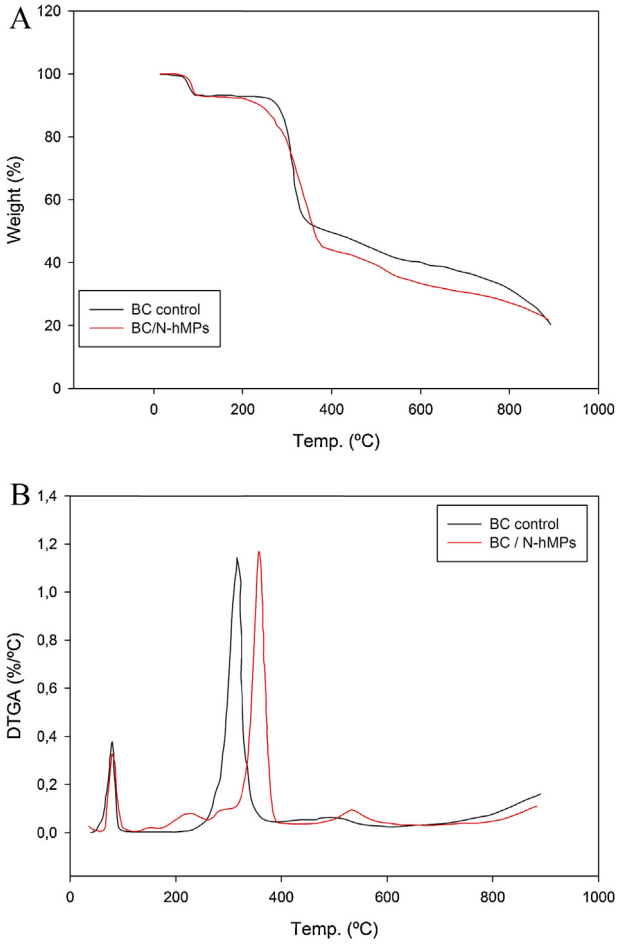

Fig. 4 – TGA (A) and DTGA (B) curves for native BC and BC/N-hMPs.

the Dox can be detected (data not shown). On the other side, the Dox is mostly located in spots when the BC membranes contain λ-Car-$CaCO_3$ indicating the advantage of the nanocomposite hybrid microparticles appended in the BC membrane surface (Fig. 5C).

Spectrophotometric fluorescence scanning of Dox confirmed similar profiles for Dox-BC samples with and without $CaCO_3$. However, Dox bathochromic maximum absorbance shift from 585 nm to 610–620 nm was observed in samples containing $CaCO_3$ suggesting an interaction between the salt and the drug (see supplementary data, Fig. 2S).

The Dox loading into the naked bacterial cellulose membrane was only 11%, probably because of the high hydrophilicity of the drug. Cellulose is a biopolymer made of β(1→4) linked D-glucose, displaying six free hydroxyls per cellobiose unit. To increase of the BC hydrophilicity through the addition of polar molecule such as λ-Car, which is containing three sulfonate groups per dimer, the Dox loading rose up to 16.6% (Fig. 6). However, the Dox loading is still very poor in both cases. In order to increase the Dox loading into the BC system, the effect of biomimetic $CaCO_3$ microparticles was considered an alternative based on the positive effect of ionic groups. The presence of $CaCO_3$ and λ-Car-$CaCO_3$ hybrid microparticles in the BC films rises up to 83.3% and 87.3% Dox loaded into hybrid BCs respectively (Fig. 6). The high Dox incorporation into the BC system attributed to the presence of $CaCO_3$-microparticles is confirming the hypothesis of the role of polar interactions between Dox and the matrix system. Despite of the 4.3% of Dox loading increase into the BC membrane in the presence of λ-Car, the BC-$CaCO_3$ and BC-λ-Car-$CaCO_3$ matrices showed statistically significant ($p \leq 0.05$) differences analyzed by the *T*-test. Incorporation of λ-Car into the BC matrix slightly increases the amount of adsorbed Dox on the BC but without control of the drug kinetic release. However, the presence of λ-Car enhances the microparticle stability on the shelf for more than one year similarly as previously reported by our laboratory (data not shown) (Bosio et al., 2014).

Dox kinetic release from the all BC matrices was first performed under normal physiological conditions in PBS (pH 7.4) at 37 °C (Table 1). Roughly, Dox released from the four matrices can be classified in two main groups based on high and low Dox release kinetics. In both groups, Dox release can be correlated to the absence or presence of microparticles in the matrix respectively. The presence of $CaCO_3$ microparticles in the matrix with and without λ-Car decreased Dox release per day in approximately 88–93% (Table 1). The results are indicative of the effect of λ-Car-$CaCO_3$ hybrid microparticles in the BC films which drastically decreases Dox release (Table 1). In addition, presence of N-hMPs on BC membranes increase the Dox loading as it was showed in the images obtained by confocal microscopy (Fig. 5). The N-hMPs works as "core" for Dox encapsulation by the interaction between the biopolymers (λ-Car and free cellulose chains) and the drug priming, the $CaCO_3$ nucleation as vaterite polymorphism (data not shown) (Kapuscinski et al., 2002). This hypothesis was confirmed by the distribution of Dox fluorescence in the images. BC samples without $CaCO_3$ displayed homogenous fluorescence covering the whole matrix surface; meanwhile matrices containing $CaCO_3$ microparticles showed intense localized Dox fluorescence dots. Additionally, Dox fluorescence intensities increase by the presence of λ-Car in the BC matrices confirmed the results displayed in Fig. 6. Besides, no Dox can be seen outside the fluorescent dots in matrices containing nanostructured λ-Car-$CaCO_3$ microparticles (N-hMPs).

The main interactions of Dox and matrix components can be attributed to the hydrogen bridges formation determined by FTIR, besides the probable interactions between aromatic rings and some hydrophobic regions of the cellulose matrix. Dox-BC stretching shifts of O–H, C–O–C and aromatic rings were observed at 3345, 1280 and 1429 cm^{-1} respectively. Also, N-H wagging shift at 873 cm^{-1} was observed for the Dox-BC. Similar shifts stretching for O–H and C–O–C groups were found for the Car-BC interactions. Particularly, the O–H stretching of BC at 3345 cm^{-1} is affected by the other molecules present in the matrices: presence of λ-Car displaced the peak to 3409 cm^{-1}, and stronger shift is observed by the addition of $CaCO_3$ to 3371 cm^{-1}. Interestingly, the phenyl breathing modes of Dox is affected by the presence of λ-Car and/or BC-λ-Car, but addition of $CaCO_3$ to the BC-λ-Car matrix showed no shift in the aromatic band indicating no hydrophobic interaction with the polymeric matrix. This result is in agreement with the confocal

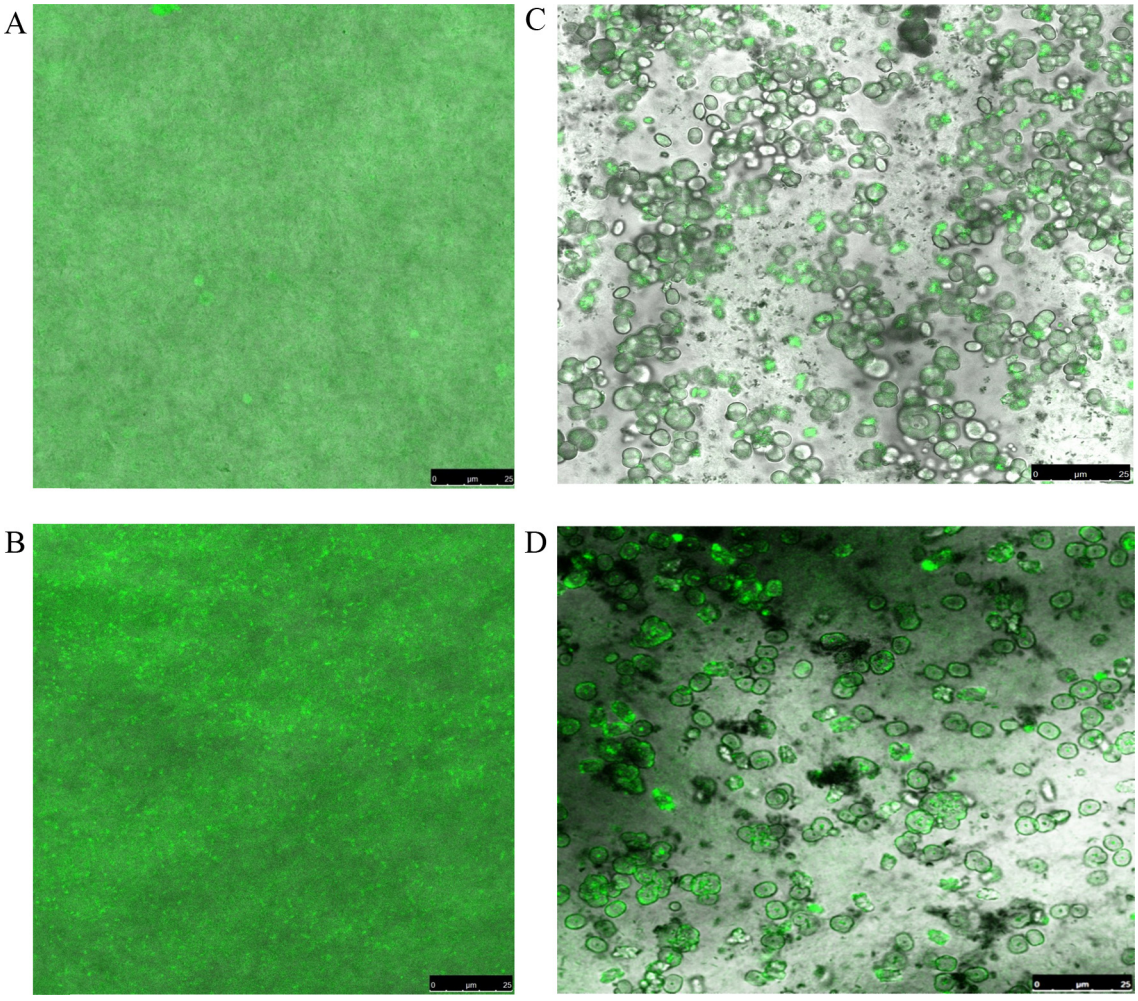

Fig. 5 – Confocal microscopy images of different BC membranes loaded with doxorubicin: (A) BC; (B) BC-λ-Car; (C) BC-$CaCO_3$; (D) BC/N-hMPs.

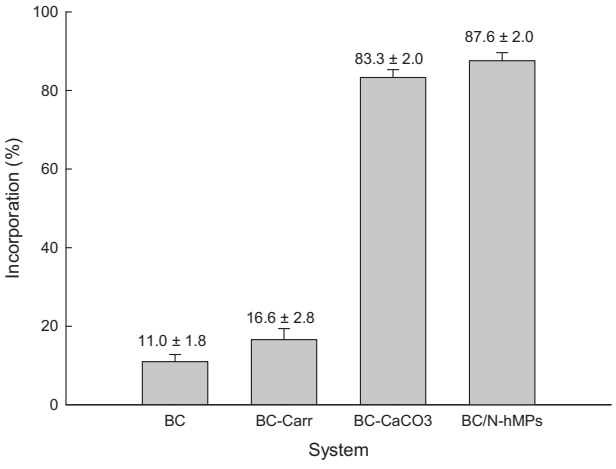

Fig. 6 – Dox binding to bacterial cellulose (BC), naked and supplemented with carrageenan, $CaCO_3$, and carrageenan plus $CaCO_3$ (N-hMPs).

microscopy pictures in where the Dox was found located principally inside the microcrystalline $CaCO_3$.

The drug loading capacity of BC-N-hMPs films was tested ranging from 258.6 to 2586.3 nmols ml^{-1} Dox initial concentrations (Fig. 7). The results showed that the amount of encapsulated drug in the hybrid film system increases linearly with Dox concentrations in the range of 258.6–2586.3 nmols ml^{-1} ($r^2 = 0.997$). Also, the amount of Dox incorporated into the BC-λ-Car-$CaCO_3$ was close to 80% for the

Table 1 – Release of doxorubicin from microbial cellulose matrices with and without $CaCO_3$ and carragenin in PBS at 37 °C for 24 h.

Matrix	Dox release (%)
BC	15.95 ± 1.86[a]
BC-Carr	12.63 ± 2.41[a]
BC-$CaCO_3$	1.32 ± 0.10
BC/N-hMPs	1.72 ± 0.15

[a] Statistically significant.

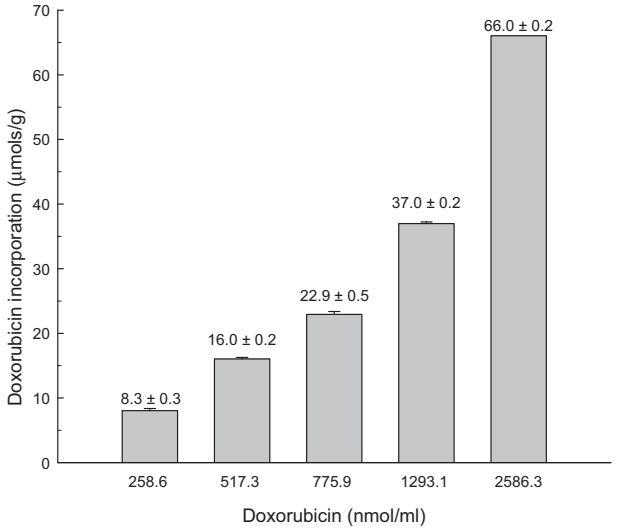

Fig. 7 – Relationship between Dox initial stock solution and BC/N-hMPs microparticles loading.

all tested concentrations. Besides, a rise of about 15% Dox encapsulation is observed at the highest drug concentration tested (2586.3 nmols ml^{-1}) which can be probably associated to the π–π stacking phenomenon of Dox aromatic rings (Bosio et al., 2014). The increase of Dox encapsulation inside N-HMPs can be inversely correlated with Dox release from the matrix (Fig. 7). This relationship is linear in the interval of 8.3–22.9 μmol μg^{-1} Dox/matrix but not at higher Dox concentrations tested of 37.0 μmol μg^{-1} and 66.0 μmol μg^{-1} (Fig. 8). Using similar range of Dox, a positive result using humanized orthotopic tumor model treated with 69 μmol μg^{-1} of Dox/silk film for local application was reported (Seib and Kaplan, 2012).

Kinetics of Dox release from BC-λ-Car-$CaCO_3$ membrane containing different amounts of drug cargo were followed in PBS (pH 7.4) for 7 days (Fig. 9). Hyperbolic curves were observed in all cases and very stable systems after 24 h. The bulk Dox release in the first part of the curve can be considered related to the Dox present in the surface and close to in the hybrid microparticles. Later, phosphate ions in the PBS solution are able to form complexes with Ca(II) present in the hybrid microparticles and the complex formation is favored since the Kps of $Ca_3(PO_4)_2$ is about 2.0×10^{-29} meanwhile the Kps for $CaCO_3$ and $CaSO_4$ are $(3.36–6.0) \times 10^{-9}$ (for calcite and aragonite, respectively) and 4.93×10^{-5} (assuming similar order of calcium sulfonate) respectively. The differences between the Kps could be roughly considered to be at least in the order of 10^{-20} in favor of calcium phosphate salt formation. In this case, the Dox release from the microspheres can be associated to the dissolution of the microparticles in the solution.

On the other hand, the effect of pH over the matrix and the Dox release kinetics is a very relevant factor since it could be applied as implantable drug delivery system for cancer therapy. Cancer cells have a high anaerobic metabolism because of the low oxygenation. In consequence there is a large accumulation of lactic acid and the extracellular pH diminishes down to 5.8 (Gerweck et al., 2006). Based on this consideration, the kinetic analysis of Dox release from the BC-λ-Car-$CaCO_3$ matrix was followed in the range of pH 5.8–7.4 during 28 days (Fig. 10). Dox was faster released from the hybrid film as the pH decreased. Changes of environmental pH from 7.4 to 5.8 made by the presence of tumor cells allow the increase of Dox release from the BC-λ-Car-$CaCO_3$ film in the range of 10–50%. This results can explained considering that the $CaCO_3$ vaterite crystals become less stable at lower pHs concomitantly with the increase of Dox solubility. Consequently, the N-hMP-BC films carrying Dox are able to release the drug under pathological conditions, meanwhile the Dox remains mostly in the matrix system for at least one year under normal physiological conditions. Also, the Dox sustained delivery could be extended for long periods of time since the

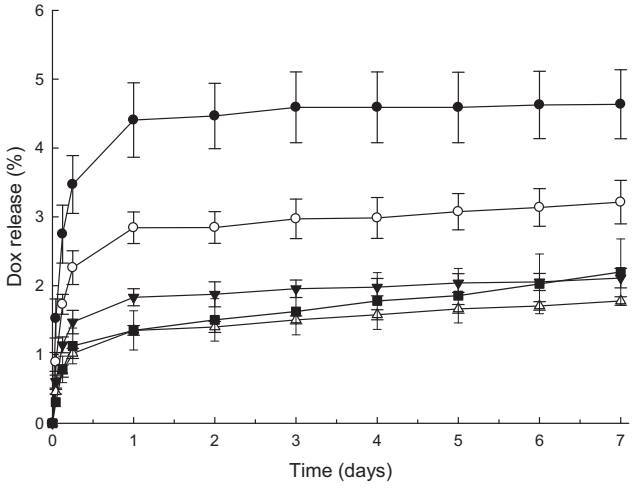

Fig. 8 – Kinetic profiles of DOX release from BC/N-hMPs containing different amount of cargo drug in PBS (pH 7.4) at 37 °C for 7 days. Symbols: ●, 8.3 μmols/g; ○, 16.0 μmols/g; ▼, 22.9 μmols/g; △, 37.0 μmols/g; ■, 66.0 μmols/g.

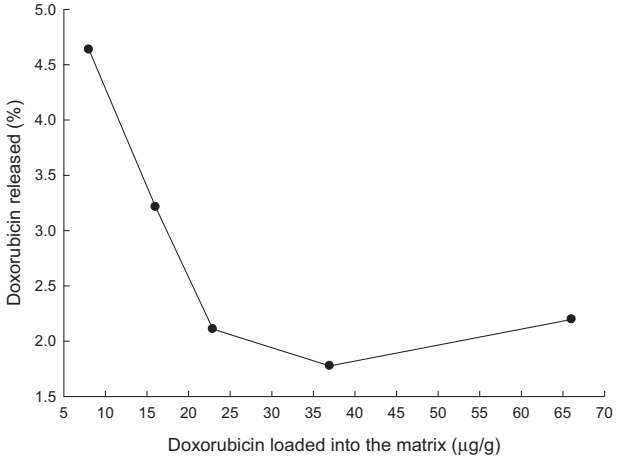

Fig. 9 – Relationship between Dox loading and release from BC/N-hMPs membranes in PBS (pH 7.4) at 37 °C for 20 h of incubation.

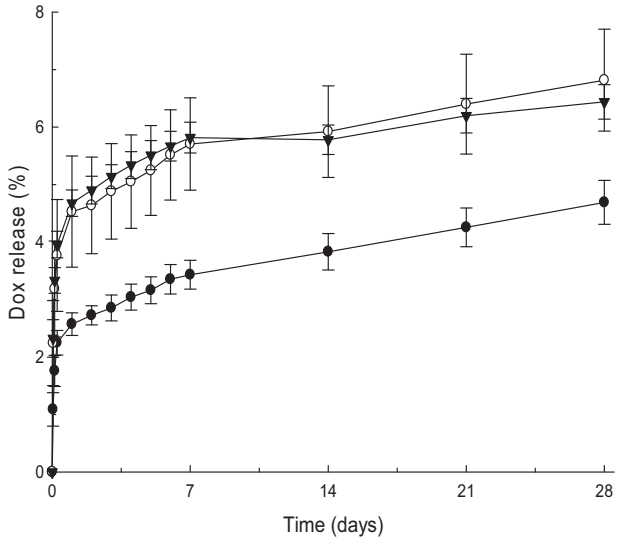

Fig. 10 – Kinetic release of BC/N-hMPs membrane loaded with 20.8 μg/g of Dox/matrix at different pH for 28 days. Symbols: ▼, pH 5.8; ○, pH 6.6; ●, pH 7.4.

Dox release was close to 7% in 28 days and 15% in one year under physiological conditions. However, further studies in normal and transformed cell cultures, different tumor models, and toxicological analysis should be performed in order to get new insights about the nanocomposite hybrid BC model.

Conclusions

In summary, the N-hMP-BC films containing Dox can be considered a smart drug delivery platform considering that the amount of the drug loading can be modulated for the development of personalized oncological treatments and the drug will be released ''on-demand'' by the reduction of local pH. Meanwhile, Dox will remain stable inside the matrix under normal physiological conditions for at least one year. Additionally, the N-hMP-BC films are made by green chemistry synthesis methods, using self-assembly techniques, and consequently scalable and from all biocompatible materials. Studies in cancer cell lines are now in course in our laboratory.

Acknowledgements

The present work was supported by the Consejo Nacional de Investigaciones Científicas y Técnicas (CONICET, PIP-0498), the Binational Argentina-Brazil grant (MINCyT-CAPES, BR/10/04), the Agencia Nacional de Promoción Científica y Técnica (ANPCyT, PICT2011-2116), and the Universidad Nacional de La Plata (11/X545) of Argentina. We are also grateful to Dr. Mario Malaspina and Dr. Natalio Kotliar from LKM Laboratories for the gift of doxorubicin used in the present work.

Appendix A. Supplementary data

Supplementary data associated with this article can be found, in the online version, at doi:10.1016/j.jab.2015.03.004.

REFERENCES

Almeida, I.F., Pereira, T., Silva, N.H., Gomes, F.P., Silvestre, A.J., Freire, C.S., Sousa Lobo, J.M., Costa, P.C., 2014. Bacterial cellulose membranes as drug delivery systems: an *in vivo* skin compatibility study. Eur. J. Pharm. Biopharm. 86, 332–336.

Anon., 2013. Paving the way for personalized medicine. In: FDA Report. .

Barud, H.S., Regiani, T., Marques, R.F.C., Lustri, W.R., Messaddeq, Y., Ribeiro, S.J., 2011. Antimicrobial bacterial cellulose-silver nanoparticles composite membranes. J. Nanomater. 11, http://dx.doi.org/10.1155/2011/721631.

Beuvier, T., Calvignac, B., Delcroix, G., Tran, M.K., Kodjikian, S., Delorme, N., Bardeau, J.F., Gibauda, A., Boury, F., 2011. Synthesis of hollow vaterite $CaCO_3$ microspheres in supercritical carbon dioxide medium. J. Mater. Chem. 21, 9757–9761.

Brito, M., Case, E., Kriven, W.M., Salem, J., Zhu, D., 2009. Use of vaterite and calcite in forming calcium phosphate cement scaffolds. Developments in porous, biological and geopolymer ceramics. Ceram. Eng. Sci. Proc. 28 (9),, http://dx.doi.org/10.1002/9780470339749.ch14.

Bosio, V.E., Cacicedo, M.L., Calvignac, B., Leon, I., Beuvier, T., Boury, F., Castro, G.R., 2014. Synthesis and characterization of $CaCO_3$-biopolymer hybrid nanoporous microparticles for controlled release of doxorubicin. Colloids Surf. B: Biointerfaces 123, 158–169.

Cai, Z.J., Hou, C.W., Yang, G., 2011. Preparation and characterization of a bacterial cellulose/chitosan composite for potential biomedical application. J. Appl. Polym. Sci. 1213, 1488–1494.

Campo, V.L., Kawano, D.F., Braz da Silva Jr., D., Carvalho, I., 2009. Carageenans: biological properties, chemical modifications and structural analysis – a review. Carbohydr. Polym. 77, 167–180.

Chiaoprakobkij, N., Sanchavanakit, N., Subbalekha, K., Pavasant, P., Phisalaphong, M., 2011. Characterization and biocompatibility of bacterial cellulose/alginate composite sponges with human keratinocytes and gingival fibroblasts. Carbohydr. Polym. 853, 548–553.

Duran Lopes, T., Riegel-Vidotti, I.C., Grein, A., Tischer, C.A., de Sousa Faria-Tischer, P.C., 2014. Bacterial cellulose and hyaluronic acid hybrid membranes: production and characterization. Int. J. Biol. Macromol. 67, 401–408.

Fernandes, S.C.M., Oliveira, L., Freire, C.S.R., Silvestre, A.J.D., Neto, C.P., Gandini, A., 2009. Novel transparent nanocomposite films based on chitosan and bacterial cellulose. Green Chem. 11, 2023–2029.

Gerweck, L.E., Vijayappa, S., Kozin, S., 2006. Tumor pH controls the *in vivo* efficacy of weak acid and base chemotherapeutics. Mol. Cancer Ther. 5, 1275–1279.

Helenius, G., Bäckdahl, H., Bodin, A., Nannmark, U., Gatenholm, P., Risberg, B., 2006. *In vivo* biocompatibility of bacterial cellulose. J. Biomed. Mater. Res. A 76, 431–438.

Islan, G.A., Cacicedo, M.L., Bosio, V.E., Castro, G.R., 2014. Development and characterization of new enzymatic modified hybrid $CaCO_3$ microparticles to obtain nano-architectured surfaces for enhanced drug loading. J. Colloid Interface Sci. 439, 76–87.

Kapuscinski, J., Ardelt, B., Piosik, J., Zdunek, M., Darzynkiewicz, Z., 2002. The modulation of the DNA-damaging effect of polycyclic aromatic agents by xanthines. Part I. Reduction of cytostatic effects of quinacrine mustard by caffeine. Biochem. Pharmacol. 63, 625–634.

Liu, X., Ma, Y., Zhou, Y., Pei, C., Yin, G., 2013. A promising hybrid scaffold material: bacterial cellulose in-situ assembling biomimetic lamellar $CaCO_3$. Mater. Lett. 102–103, 91–93.

Petersen, N., Gatenholm, P., 2011. Bacterial cellulose-based materials and medical devices: current state and perspectives. Appl. Microbiol. Biotechnol. 91, 1277–1286.

Seib, F.P., Kaplan, D.L., 2012. Doxorubicin-loaded silk films: drug-silk interactions and *in vivo* performance in human orthotopic breast cancer. Biomaterials 33, 8442–8450.

Song, G., Darr, D.B., Santos, C.M., Ross, M., Valdivia, A., Jordan, J. L., Midkiff, B.R., Cohen, S., Nikolaishvili-Feinberg, N., Miller, C.R., Tarrant, T.K., Rogers, A.B., Dudley, A.C., Perou, C.M., Zamboni, W.C., 2014. Tumor micro-environment is a rough neighborhood for nanoparticle cancer drugs. Clin. Cancer Res. 20, 6083–6095.

Stoica-Guzun, A., Stroescu, M., Jinga, S.I., Jipa, I.M., Dobre, T., 2013. Microwave assisted synthesis of bacterial cellulose-calcium carbonate composites. Ind. Crops Prod. 50, 414–422.

Svensson, A., Nicklasson, E., Harrah, T., Panilaitis, B., Kaplan, D. L., Brittberg, M., Gatenholm, P., 2005. Bacterial cellulose as a potential scaffold for tissue engineering of cartilage. Biomaterials 26, 419–431.

Tacar, O., Sriamornsak, P., Dass, C.R., 2012. Doxorubicin: an update on anticancer molecular action, toxicity and novel drug delivery systems. J. Pharm. Pharmacol. 65, 157–170.

Wolinsky, J.B., Colson, Y.L., Grinstaff, M.W., 2012. Local drug delivery strategies for cancer treatment: gels, nanoparticles, polymeric films, rods, and wafers. J. Control. Release 159, 14–26.